



HAL
open science

3D Navigation With An Insect-Inspired Autopilot

Geoffrey Portelli, Julien Serres, Franck Ruffier, Nicolas Franceschini

► **To cite this version:**

Geoffrey Portelli, Julien Serres, Franck Ruffier, Nicolas Franceschini. 3D Navigation With An Insect-Inspired Autopilot. Deuxième conférence française de Neurosciences Computationnelles, "Neuro-comp08", Oct 2008, Marseille, France. hal-00331566

HAL Id: hal-00331566

<https://hal.science/hal-00331566v1>

Submitted on 17 Oct 2008

HAL is a multi-disciplinary open access archive for the deposit and dissemination of scientific research documents, whether they are published or not. The documents may come from teaching and research institutions in France or abroad, or from public or private research centers.

L'archive ouverte pluridisciplinaire **HAL**, est destinée au dépôt et à la diffusion de documents scientifiques de niveau recherche, publiés ou non, émanant des établissements d'enseignement et de recherche français ou étrangers, des laboratoires publics ou privés.

3D NAVIGATION WITH AN INSECT-INSPIRED AUTOPILOT

G.PORTELLI, J.SERRES, F.RUFFIER, and N.FRANCESCHINI
 Institut des Sciences du Mouvement Etienne Jules Marey – UMR6233
 CP938 - 163 av de Luminy – 13009 Marseille
 France
 Email : geoffrey.portelli@univmed.fr

ABSTRACT

Using computer-simulation experiments, we developed a vision-based autopilot that enables a ‘simulated bee’ to travel along a tunnel by controlling both its speed and its clearance from the right wall, the left wall, the ground, and the ceiling. The flying agent can translate along three directions (surge, sway, and heave): the agent is therefore *fully actuated*. The visuo-motor control system, called ALIS (Autopilot using an Insect based vision System), is a *dual OF regulator* consisting of two interdependent feedback loops, each of which has its own OF set-point. The experiments show that the simulated bee navigates safely along a straight tunnel, while reacting sensibly to the major OF perturbation caused by the presence of a tapered tunnel. The visual system is minimalistic (only eight pixels) and it suffices to control the clearance from the *four walls* and the forward speed jointly, without the need to measure any speeds and distances. The OF sensors and the simple visuo-motor control system developed here are suitable for use on MAVs with avionic payloads as small as a few grams. Besides, the ALIS autopilot accounts remarkably for the quantitative results of ethological experiments performed on honeybees flying freely in straight or tapered corridors.

KEYWORDS

Optic flow, autopilot, bionics, biorobotics, biomimetics.

1. Introduction

Flying insects are able to navigate in unfamiliar environments by relying on the *optic flow* (OF) [1] that is generated by their own motion [2]. They rely on OF cues to avoid obstacles [3, 4], to control their speed [5, 6, 7], to control their height, and to land [6, 8, 9, 10]. Honeybees trained to fly in a narrow flight tunnel (a corridor of width $\sim 12\text{cm}$) were observed to fly close to the midline [3]. To explain this *centering response*, the authors hypothesized that the bee may balance the lateral OFs perceived on either sides [3]. Our own findings show, however, that bees flying through a wider tunnel ($\sim 95\text{cm}$) do not center systematically and can exhibit instead a *wall-following behavior* [4, 11]. We have developed an autopilot (called LORA III), based on two *lateral OF regulators*, which enables

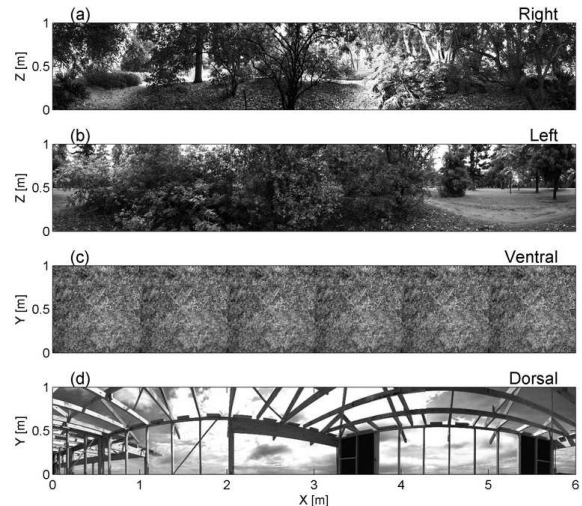


Fig. 1. The grayscale natural scenes used to wallpaper the 4 faces of the simulated tunnel. Resolution of the images is 1000×6000 pixels (1 pixel = 1mm^2). Images are therefore 1×6 -meter in size. All four faces of the tunnel are wallpapered with different images: right wall (a), left wall (b), ground (c), and ceiling (d).

an agent to control its speed and avoid lateral obstacles [12].

The aim of the present study is to extend the OF regulation hypothesis to the three dimensions (x, y, z). The newly developed autopilot, called ALIS (*Autopilot using an Insect based vision System*) [13] relies on left, right, ventral, and dorsal OF cues. We show that it enables 3D navigation in a tunnel.

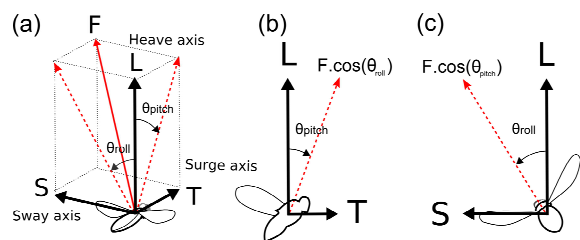


Fig. 2. (a) Resolution of the mean flight-force vector F along the surge X-axis giving the forward thrust T , along the sway Y-axis giving the side thrust S , and along the heave Z-axis giving the vertical lift L . (b) Forward thrust results from pitching the mean flight-force vector F by an angle θ_{pitch} . (c) Side thrust S results from rolling the mean flight-force vector F by an angle θ_{roll} .

2. Materials and methods

All experiments consist of computer-simulations using MatlabTM/Simulink softwares. The simulated

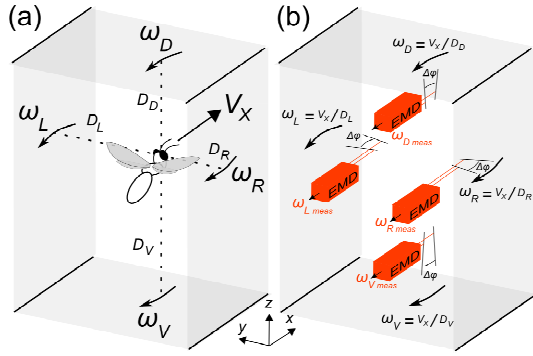


Fig. 3. (a) A simulated bee flying at forward speed V_x along a tunnel generates an OF (9) that depends on the perpendicular distance (right D_R , left D_L , ventral D_V , dorsal D_D) from the tunnel surfaces. The simulated bee is equipped with four OF sensors. The sensors' axes are maintained oriented at fixed roll and pitch orientations, perpendicular to the walls, ground and ceiling, respectively, and measure OF generated laterally (ω_L and ω_R), ventrally (ω_V) and dorsally (ω_D). (b) Each OF sensor consists of only two photoreceptors (two pixels) driving an Elementary Motion Detector (EMD). The visual axes of the two photoreceptors are separated by an interreceptor angle $\Delta\phi = 4^\circ$.

3D visual environment is a flight tunnel (6-meter long, 1-meter wide, and 1-meter high), the four walls of which are wallpapered with natural images (Fig. 1). The dynamic model of the simulated bee is described by its three translational degrees of freedom (surge, sway, and heave dynamics) (x,y,z) (Fig. 2). Pitching the mean flight-force vector F by an angle θ_{pitch} generates a forward thrust T [14]. Rolling the mean flight-force vector F by an angle θ_{roll} generates a side thrust S . Lift production depends on the wing stroke amplitude [15]. The bee's head orientation is assumed to be locked to the tunnel X-axis, so that it will perceive only purely translational OFs [16]. The bee is equipped with four OF sensors (two lateral, one ventral, and one dorsal, Fig. 3a). Each OF sensor is an Elementary Motion Detector (EMD) driven by two photoreceptors (two pixels), whose visual axes are separated by an interreceptor angle $\Delta\phi = 4^\circ$ (Fig. 3b). Each photoreceptor angular sensitivity is a bell-shaped function with an acceptance angle (angular width at half height) $\Delta\rho = 4^\circ$ as well ($\Delta\rho/\Delta\phi = 1$). The photoreceptor output is computed at each time step (1ms) by convolving the natural scene with a 2D Gaussian filter that mimics the (insect-like) photoreceptor Gaussian sensitivity (Fig. 4). The ALIS autopilot that drives the simulated bee combines the OCTAVE autopilot (for ground avoidance [17]) and the LORA III autopilot (for speed control and lateral obstacle avoidance [12]). The ALIS autopilot consists of two visuomotor feedback loops: the *speed control* loop (along the surge axis) and the *positioning control*

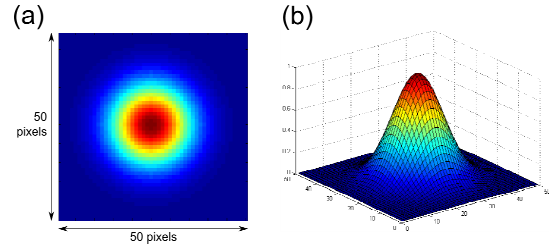


Fig. 4. (a) Spatial convolution matrix that represents a Gaussian filter at 25cm from the walls. Each photoreceptor angular sensitivity is a Gaussian function with an acceptance angle (angular width at half height) $\Delta\rho = 4^\circ$. The photoreceptor output is computed at each time step (1ms) by convolving the natural scene with a 2D Gaussian filter that mimics the photoreceptor Gaussian sensitivity. The Gaussian filter is calculated depending on the distance from the wall. (b) 3D view of the same Gaussian filter.

loop (along both the sway and heave axes). Both loops operate in parallel and are intertwined. Each of them involves multiple processing stages, each one has its own OF set-point: the *forward OF set-point* and the *positioning OF set-point*.

3. Results

The simulated environment is a straight tunnel - 6-meter long, 1-meter wide, and 1-meter high (Fig. 5). Walls, ground, and ceiling are wallpapered with natural images, as shown in the perspective view (Fig. 5a). The simulated bee enters the tunnel at initial coordinates $x_0=0.1m$, $y_0=0.15m$, $z_0=0.15m$, and with an initial speed $V_{x0}=0.2m/s$ (Fig. 5b). Figure 5c shows the trajectory projection in the horizontal plane (x,y) and figure 5d in the vertical plane (x,z) . The simulated bee can be seen to gradually increase both its height of flight (Fig. 5d) and its right clearance to 0.33m (Fig. 5c), while the forward speed automatically increases to 2m/s, i.e., to the maximal speed allowed (Fig. 5e). By selecting the highest value of the four EMD outputs (Fig. 5f), the positioning control loop commands either the heave or sway dynamics at a time, making the bee avoid both the ground and the right wall. In the steady state, the simulated bee can be seen to reach a ventral and a right OF measured ($\omega_{Vmeas}=\omega_{Rmeas}=2.48V$, i.e., $355^\circ/s$) that are both close to the positioning OF set-point (set to 2.4V, i.e., $315^\circ/s$). The speed achieved is close to saturation. The forward feedback signal reaches 4.42V ($525^\circ/s$) in Fig. 5g, which is close to the forward OF set-point (set to 4.57V, i.e., $540^\circ/s$).

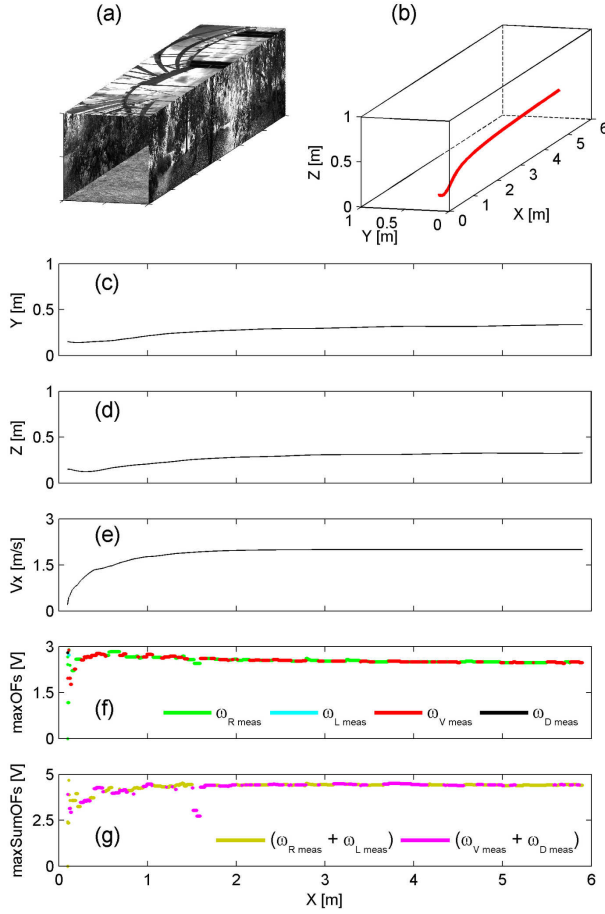


Fig. 5. (a) Perspective view of the straight flight tunnel. (b) Simulated bee's 3D trajectory starting at $x_0=0.1\text{m}$, $y_0=-0.15\text{m}$, $z_0=0.15\text{m}$ with initial speed $V_{x0}=0.2\text{m/s}$. (c) Flight track in the horizontal plane (x,y). (d) Flight track in the vertical plane (x,z). (e) Forward speed V_x profile. (f) Positioning feedback signal (equal to the *maximum output* of the four OFs sensors: right OF sensor = green; left OF sensor = cyan; ventral OF sensor = red; dorsal OF sensor = black). (g) Forward feedback signal (equal to the *maximum of the sum* of the two coplanar OFs measured: horizontal OF sensors = yellow; vertical OF sensors = magenta).

In figure 6, the simulated tunnel is a 6-meter long, 1-meter high tapered tunnel (tapering angle 7°) with a 1-meter wide entrance and a 0.25-meter wide constriction located midway (Fig. 6a). This tunnel is designed to test the ALIS autopilot in its ability to reject a strong lateral OF disturbance. The simulated bee enters the tunnel at initial coordinates $x_0=0.1\text{m}$, $y_0=0.85\text{m}$, $z_0=0.6\text{m}$ and with an initial speed $V_{x0}=0.2\text{m/s}$ (Fig. 6b). Figure 6c shows the trajectory in the horizontal plane (x,y) and figure 6d in the vertical plane (x,z). The simulated bee can be seen to automatically slow down as it approaches the narrowest section of the tapered tunnel, and to accelerate again when the tunnel widens beyond it (Fig. 6e). The positioning feedback signal (Fig. 6f) can be seen to have selected the left measured OF, which appears to be maintained close to the positioning OF set-point throughout the trajectory (Fig. 6f). The simulated bee can be seen to follow

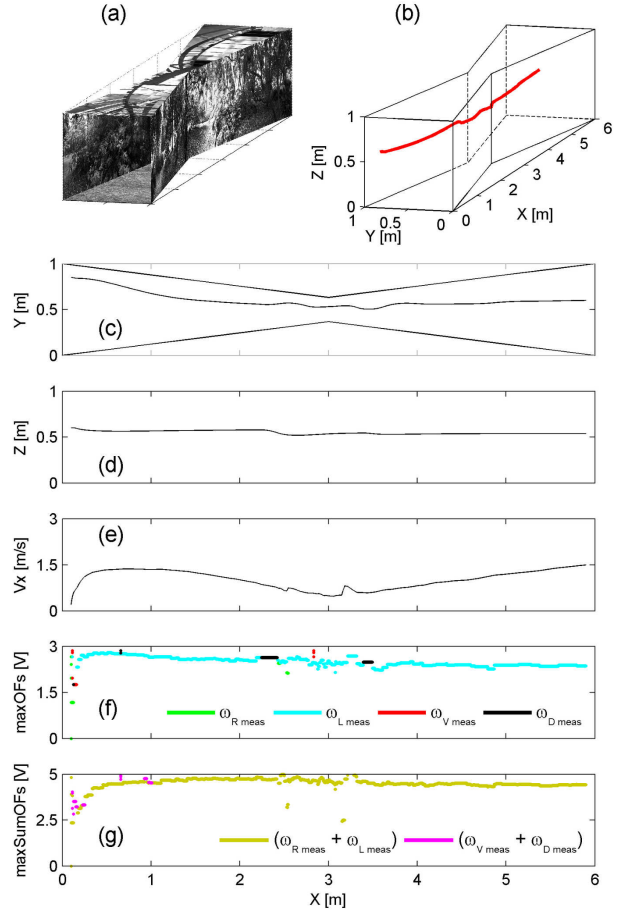


Fig. 6. (a) Perspective view of the tapered tunnel. (b) Simulated bee's 3D trajectory starting at initial coordinates $x_0=0.1\text{m}$, $y_0=0.85\text{m}$, $z_0=0.6\text{m}$, with initial speed $V_{x0}=0.2\text{m/s}$. (c) Trajectory in the horizontal plane (x,y). (d) Trajectory in the vertical plane (x,z). (e) Forward speed V_x profile. (f) Positioning feedback signal defined as the maximum output of the four OFs sensors (right OF sensor = green; left OF sensor = cyan; ventral OF sensor = red; dorsal OF sensor = black). (g) Forward feedback signal defined as the maximum of the sum of the two coplanar OFs measured (horizontal OF sensors = yellow; vertical OF sensors = magenta).

the left wall of the tapered tunnel. The reason is simply that its initial position was close to that wall. Since the tunnel narrows only in the horizontal plane, the OF in the *vertical* plane is of little concern to the ALIS autopilot (Fig. 6g). The simulated bee can be seen to cross the tapered tunnel without being dramatically disturbed by major right and left OFs disturbances.

4. Conclusion

Results show that the ALIS autopilot suffices to make a bee navigate safely *under exclusively visual control* along a straight tunnel (Fig. 5) and even along a tapered tunnel (Fig. 6). The visual system involved in these experiments is minimalistic and consists of only eight pixels forming four EMDs (two EMDs in the horizontal plane, two EMDs in the vertical plane). The ALIS autopilot enables the

agent to perform obstacle avoidance using maneuvers that involve *translational* DOF exclusively, unlike obstacle avoidance based on body saccades, which involve rotational DOFs [18]. Key to the working of the ALIS autopilot is a pair of *OF regulators* that aim at maintaining the perceived OF constant by acting upon the forward, lateral, and vertical thrusts. The great advantage of this visuomotor control system is that it leads to a given speed and a given distance to the walls without having to *measure* any speeds and distances.

In spite of the very low number (four) of OF sensors involved (one on the right, one on the left, one underneath, and one on the top: Fig. 3) the ALIS autopilot accounts remarkably well for behaviors observed in real bees that were trained to fly along various, stationary [3-4,7] or tapered corridors [6]. One may therefore reasonably assume that bees are equipped with an ALIS-like *dual OF regulator* – a control system that is, in addition, little demanding in terms of neural computation. ALIS autopilot operates without any needs for velocimeters and range sensors. Visual-control systems based on insects studies can yield solutions that are efficient and little demanding in terms of computation. These biomimetic solutions pave the way for the design of lightweight and low-cost visual guidance systems for autonomous robots, with potential applications to both aerospace and undersea vehicles.

References :

- [1] J.J. Gibson, "The perception of the visual world," Boston: Houghton Mifflin, 1950.
- [2] G.A. Horridge, "The evolution of visual processing and the construction of seeing system," *Proc. Roy. Soc. Lond. B*, vol. 230, pp. 279-292, 1987.
- [3] M.V. Srinivasan, M. Lehrer, W.H. Kirchner, and S.W. Zhang, "Range perception through apparent image speed in freely flying honeybees," *Vis. Neurosci.*, vol. 6, pp. 519-535, 1991.
- [4] J. Serres, F. Ruffier, G.P. Masson, and N. Franceschini, "A bee in the corridor: centering or wall-following?," In *Proc. of the 7th meeting of the German neuroscience society - 31st Göttingen neurobiology conference*, Göttingen, Germany, T14-8B, 2007.
- [5] R. Preiss, "Motion parallax and figural properties of depth control flight speed in an insect," *Biol. Cyb.*, vol. 57, pp. 1-9, 1987.
- [6] M.V. Srinivasan, S.W. Zhang, M. Lehrer, and T.S. Collett, "Honeybee navigation. en route to the goal: visual flight control and odometry," *J. Exp. Biol.*, vol. 199, pp. 237-244, 1996.
- [7] E. Baird, M.V. Srinivasan, S. Zhang, and A. Cowling, "Visual control of flight speed in honeybees," *J. Exp. Biol.*, vol. 208, pp. 3895-3905, 2005.
- [8] M. V. Srinivasan, S.W. Zhang, J.S. Chahl, E. Barth, and S.Venkatesh, "How honeybees make grazing landings on flat surfaces," *Biol. Cyb.*, vol. 83, pp. 171-183, 2000.
- [9] E. Baird, M.V. Srinivasan, S. Zhang, R. Lamont, and A. Cowling, "Visual control of flight speed and height in honeybee," *LNAI*, vol. 4095, pp. 40-51, 2006.
- [10] N. Franceschini, F. Ruffier, and J. Serres, "A bio-inspired flying robot sheds light on insect piloting abilities," *Current Biology*, vol. 17, pp. 329-335, 2007.
- [11] J. Serres, G. Masson, F. Ruffier, and N. Franceschini "A bee in the corridor: centring and wall-following," *Naturwissenschaften*, en révision, 2008.
- [12] J. Serres, D. Dray, F. Ruffier, and N. Franceschini, "A vision-based autopilot for a miniature air-vehicle: joint speed control and lateral obstacle avoidance," *Autonomous Robot*, vol. 25 pp. 103 -122, 2008.
- [13] G. Portelli, J. Serres, F. Ruffier, and N. Franceschini, "An insect-inspired visual autopilot for corridor-following," submitted, 2008.
- [14] C. David, "The relationship between body angle and flight speed in free-flying *Drosophila*," *Physiol. Entomol.*, vol. 3, pp. 191-195, 1978.
- [15] S.P. Sane and M.H. Dickinson, "The aerodynamic effects of wing rotation and a revised quasi-steady model of flapping flight," *J. Exp. Biol.*, vol. 205, pp.1087-1096, 2002.
- [16] J. Zeil, N. Boeddeker, and J.M. Hemmi, *Visually guided behavior* (New Encyclopedia of Neuroscience, Amsterdam: Elsevier Science Publishers), in press, 2008.
- [17] F. Ruffier and N. Franceschini, "Optic flow regulation: the key to aircraft automatic guidance," *Robotics and Autonomous Systems*, vol. 50(4), pp. 177-194, 2005.
- [18] A. Beyeler, J.-C. Zufferey, and D. Floreano, "3D vision-based navigation for indoor microflyers," in *Proc. IEEE int. conf. on robotics and automation, ICRA*, pp. 1336-1341, 2007.